1998

Error characterization of the alpha residuals emissivity extraction technique

Michael Baglivio

Senior Research

Error Characterization of the Alpha Residuals Emissivity Extraction Technique

Final Report

Michael C. Baglivio
Center for Imaging Science
Rochester Institute of Technology
May 1998

Table of Contents

Error Characterization of the Alpha Residuals Emissivity Extraction Technique

Michael C. Baglivio

Table of Contents

Title Page

Error Characterization of the Alpha Residuals Emissivity Extraction Technique

Michael C. Baglivio

Abstract

When dealing with remotely sensed images, a parameter that aids in material identification is its emissivity. By extracting a materials emissivity spectrum, the probability of correctly identifying it greatly increases. The Alpha Residual algorithm was developed for just such a process.

The Alpha Residuals emissivity extraction technique was originally developed for six channel Thermal Infrared Multispectral Scanner (TIMS) data. In dealing with TIMS data, it is known that the error at 300K is 1%. In recent years, detector technology has led to sensors with higher spectral resolution and an increased number of bands. The goal of this project is to determine if error is reduced due to increased spectral resolution and to produce an error plot that is temperature dependent.

An error characterization algorithm was written in C++ to simulate one pixel in a 128-channel Spatially Enhanced Broadband Array Spectrograph System (SEBASS) image with known output. After the results for this were validated, the algorithm was applied to real data. Spectral response and the number of sample points per channel were shown to contribute to the resulting amount of error. As the number of sample points per channel increased, the error between the two alpha residual spectra decreased. When spectral response width increased, so did the error. When actual image data was used, the error had significant spectral structure, but was still very small. This technique is a pixel by pixel operation and thus, outputs an error spectrum for each pixel.

Table of Contents

Center for Imaging Science
Rochester Institute of Technology
Rochester, NY 14623-5604

This report is accepted in partial fulfillment of the requirements of the course SIMG-503 Senior Research.

Title: Error Characterization of the Alpha Residuals Emissivity Extraction Technique
Author: Michael C. Baglivio
Project Advisor: Dr. John Schott, Scott Brown
SIMG 503 Instructor: Joseph P. Hornak

Table of Contents

Error Characterization of the Alpha Residuals Emissivity Extraction Technique

Michael C. Baglivio

Acknowledgement

First, I would like to thank my mother, Margaret McAdorey. Her love and support has made the bad times good and the good times better. Witout her, my education at RIT would not have been possible.

I would also like to thank Scott Brown, who took the small amount of spare time he had throughout the year to help myself and other seniors with our projects.

Table of Contents

Error Characterization of the Alpha Residuals Emissivity Extraction Technique

Michael C. Baglivio

Introduction

The hypothesis to be tested in this research is that an error spectrum can be generated and applied to real and synthetic imagery to correctly estimate target spectral emissivity. Implementation of this technique spans many applications from environmental to military. Being able to separate out emissivity spectra increases our ability to identify what we're looking at. Without this knowledge, different materials can be mistaken for one another. Upon successful characterization of these algorithms and the genre they're best suited for, environmental uses would include identifying how much of a specific chemical is polluting some given body of water based on spectral characteristics of the pollutant. Utilization in the military field includes identification of enemy vehicles based on the content of the paint used on their vehicles. Other applications would be in monitoring soil and vegetation interaction in the agricultural areas of the world. Analysis of volcanic processes can also be achieved by data output by separation techniques. (1)

Other areas of interest for this study include effects of the frequency of the input on the resulting error. Do high frequency emissivity spectra yield a significant difference in error than low frequency spectra? How does spectral response width of each band of the sensor effect error? Does varying the width of this approximately Gaussian response effect the output? What if the sensor has a high spectral resolution? Does that minimize error? How does the number of sample points taken in each band effect the error? Answers for all these questions will be provided throughout the course of this thesis.

Background

Governing Equation

Temperature and emissivity values are extracted from the thermal infrared region of the spectrum. Both of these values contribute to the spectral radiance seen by the sensor as shown in the following equation.

$$L_\lambda = \left\{ \begin{matrix} E'_{s\lambda} \cos(\sigma) \tau_1(\lambda) \frac{r(\lambda)}{\pi} + \varepsilon(\lambda) L_{T\lambda} + F\left[E_{ds\lambda} + E_{d\varepsilon\lambda}\right] \frac{r_d(\lambda)}{\pi} \\ + (1-F)\left[L_{\vartheta s\lambda} + L_{\vartheta\varepsilon\lambda}\right] r_d(\lambda) \end{matrix} \right\} \tau_2(\lambda) + L_{us\lambda} + L_{u\varepsilon\lambda}$$

This is the governing equation that defines the amount of radiance reaching a sensor. $E'_{s\lambda}$ is the exoatmospheric solar irradiance, σ is the declination angle from the normal to the sun, τ_1 is the path transmission from the sun to the target, $r_d(\lambda)/\pi$ is the bi-directional reflectance factor, $\varepsilon(\lambda)$ is the spectral emissivity, $L_{T\lambda}$ is the target thermal radiance due to temperature, F is the shape factor which defines how much sky the target is exposed to, $E_{ds\lambda}$ is the scattered irradiance from the sun hitting the target, $E_{d\varepsilon\lambda}$ is

the self emitted irradiance from the atmosphere that hits the target, $L_{ds\lambda}$ is the radiance from the sun reflected of surrounding objects and the target, $L_{d\varepsilon\lambda}$ is the radiance from photons being self emitted from surround objects and reflected off the target, $L_{us\lambda}$ is the upwelled radiance from photons leaving the sum, and $L_{d\varepsilon\lambda}$ is the thermal self-emitted radiance from the atmosphere. $\tau_2(\lambda)$ is the target to sensor transmission. (2)

It is the photons that are self-emitted by the target that are of interest in this study. These photons are given by the term $\varepsilon(\lambda)L_{Tl}\tau_2(\lambda)$. The spectral emissivity term is lumped in with wavelength dependent thermal radiance and target sensor transmission. Multiplying these three values produces the contribution to total radiance from the targets self-emitted photons. Our goal is to determine how much of this contribution is due to its emissivity.

Blackbody Equation

A blackbody is defined as an idealized surface or cavity that has the property that all incident electromagnetic flux is perfectly absorbed and then re-radiated (2). A blackbody is defined by Planck's equation:

$$M_\lambda = 2\pi hc^2\lambda^{-5}(e^{\frac{hc}{\lambda kT}} - 1)^{-1}$$

Where h is Planck's constant, c is the speed of light, k is the Boltzman constant, and T is temperature in degrees Kelvin. An object whose emissivity is approximately constant with wavelength is called a gray body while objects with varying emissivities are called selective radiators. Most materials could be classified under this category because their emissivity changes with wavelength.

Emissivity

Temperature of an object results from self-emitted photons. These self emitted photons are the only source of information for an object's temperature (2). Emissivity is defined as the ratio of spectral exitance $M_\lambda(T)$ from an object at temperature T (in Kelvins) to the exitance from a blackbody at that same temperature $M_{\lambda BB}(T)$ or:

$$\varepsilon(\lambda) = \frac{M_\lambda(T)}{M_{\lambda BB}(T)}$$

Significant Equations

Prior to the use of actual data, there are many equations used to simulate and manipulate data that will be used throughout the course of this study. First we need to simulate some input data, $L(\lambda)$. This is done by multiplying Planck's curve by a known emissivity.

Where L_{BBT} is a blackbody at a given temperature and $\varepsilon(\lambda)$ is the spectral emissivity.

Next we need to compute a sensor radiance that will take into account the number of sample

points being used, the spectral responsivity of the sensor, and the spectral radiance. Convolving the spectral responsivity with a kernel of size sample points containing spectral radiance values does this. The equation is given by:

Where $L_{\lambda i}$ is the integrated sensor radiance, $\beta(\lambda)$ is the spectral responsivity, and $L(\lambda)$ is the simulated spectral radiance.

Similarly to this, an effective emissivity must be computed by degrading to the spectral bandwidth of each channel. This is given by:

$$\varepsilon_{\lambda_i} = \frac{\int \varepsilon(\lambda)\beta(\lambda)d\lambda}{\int \beta(\lambda)d\lambda}$$

Alpha Residuals

The alpha residuals is an algorithm published by Simon Hook of the Jet Propulsion Laboratory (JPL) at the California Institute of Technology. It was originally developed for Thermal Infrared Multispectral Scanner (TIMS) data, but it will be applied to SEBASS data here. The alpha residual equations are derived from Wein's approximation of the blackbody equation and that is believed to be the source of its error. When applying it to an image, there are no surround effects because it only operates on one pixel at a time. For each band of a sensor, a single alpha residual value is computed. After being computed for all bands, an alpha residual spectrum can be produced. It approximates the shape of that pixels emissivity spectrum. This is done for image data first with the following equations.

$$X_i = \lambda_i \ln L_{\lambda i}$$

$$\overline{X_i} = \overline{\lambda_i \ln L_{\lambda i}}$$

$$\alpha_i = X_i - \overline{X_i}$$

λ_i is the central bandwidth of the channel and α_i is the alpha residual for that channel.

Next, an alpha residual is computed for library data. Library data is in the form of emissivity spectra. These emissivity spectra are plugged in to the following equations to produce a library alpha residual spectrum. Be sure to observe that the emissivity values used in this equation are effective emissivites from the equation given earlier.

$$X_i = \lambda_i \ln \varepsilon_i + \lambda_i \ln C_1 - 5\lambda_i \ln \lambda_i - \lambda_i \ln \pi - \frac{C_2}{T}$$

$$\overline{X_i} = \frac{\sum \lambda_i \ln \varepsilon_i}{N} + \frac{\sum \lambda_i \ln C_1}{N} - \frac{\sum 5\lambda_i \ln \lambda_i}{N} - \frac{\sum \lambda_i \ln \pi}{N} - \frac{C_2}{T}$$

$$\alpha_i = X_i - \overline{X_i}$$

N is the number of spectral bands, $C_1=2\pi hc^2$, and $C_2=hc/\lambda$ where h is Planck's constant, c is the speed of light, and k is Boltzmann's constant.

After both alpha residual spectra are computed, their shapes are compared. A pixel gets assigned the library emissivity that produced the alpha residual spectrum that is most similar to the alpha residual spectrum of the image data. This is done for each pixel in the image so that each one has a specific emissivity. (3)

The SEBASS Sensor

The Spatially Enhanced Broadband Array Spectrograph (SEBASS) sensor is a hyperspectral infrared airborne sensor. It's operating altitude ranges from 2,000 to 12,500 feet. Pixel sizes (ground sample distance) range from 2 to 12.5 feet. SEBASS scans over the mid wave infrared (MWIR) and long wave infrared (LWIR) which have 128 spectral channels each. The MWIR ranges from 2μm to 5.2 μm while the LWIR ranges from 7.8μm to 13.4μm. Bandwidths (Dl for the MWIR and LWIR are 0.025 and »0.04 respectively. It contains a push-broom sensor. A push-broom sensor utilizes a linear array of detectors and collects entire lines of data. Ground cover by this detector is dependent on the size of the array. There are no moveable parts so ground swath is decreased. The benefit of this is that it can increase the lifespan of the instrument, but as mentioned earlier, significantly decreases the amount of data you can collect compared to sensors with mobile optics. (3)

Computer Code

The main tool to be used throughout this study is a C++ program that will be written for the specific needs of this research. User will supply input such as the name of the emissivity file to be used, temperature range for data to be computed, number of sample points to be used, width of spectral responsivity curve, and the name of the output file.

Methods

Frequency Effects

The first step in this research is to determine the effect of frequency of input on the resulting error. To do this, three pseudo-emissivity curves will be generated with cosine waves of varying frequency. These cosine waves must be scaled and shifted to properly simulate actual emissivities. The equation to

be used is:

$$\varepsilon_i = 0.975 + 0.25\cos(\frac{i}{f}) \qquad i = 0,1,2,\ldots n \qquad f = 5,10,20$$

Where i is the index, f is the period, and n is the total number of points. Multiplying these pseudo-emissivity spectra with blackbody curves at varying temperatures will simulate input data. These curves will be generated in the C ++ code that is to be written. After results are obtained for all three spectra, files will be generated and then read in by the code so validation of correctly reading in data is achieved before the next step. If the data is correctly read in, the results will be the same as when the emissivity was generated within the program. This will give us more confidence in the results obtained when actual emissivity spectra files are read in.

Effect of Sampling and Response Width

Upon completion of the previous step, simulated emissivity files will be replaced with actual ones. All combinations of 1, 3, and 5 sample points and spectral response widths of 5, 7, and 9 will be used to determine each parameter's contribution to error. These combinations will also be tested on multiple material's emissivity to see if there is an optimal combination from material to material or a general sample point and response width relationship for all materials.

Error Correction

The final goal of this project is to find a general error correction that can be applied to reduce or eliminate error. This will be done by taking the spectral difference of the image alpha residuals and the library alpha residuals. Doing this will yield the difference of the alpha residual in each band. It is hopeful that by adjusting the image alpha residuals by the inverse of the difference will greatly compensate for any inconsistencies.

Results

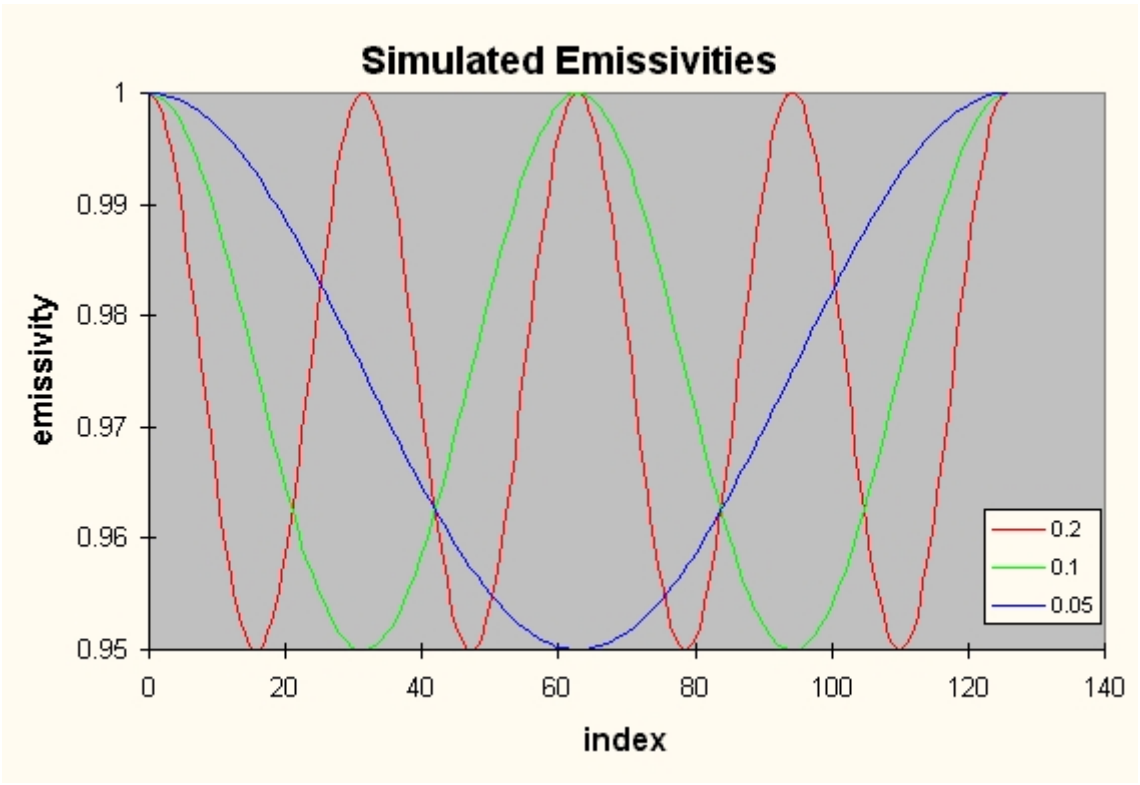

Figure 1: *Simulated Input Emissivities for frequency study*

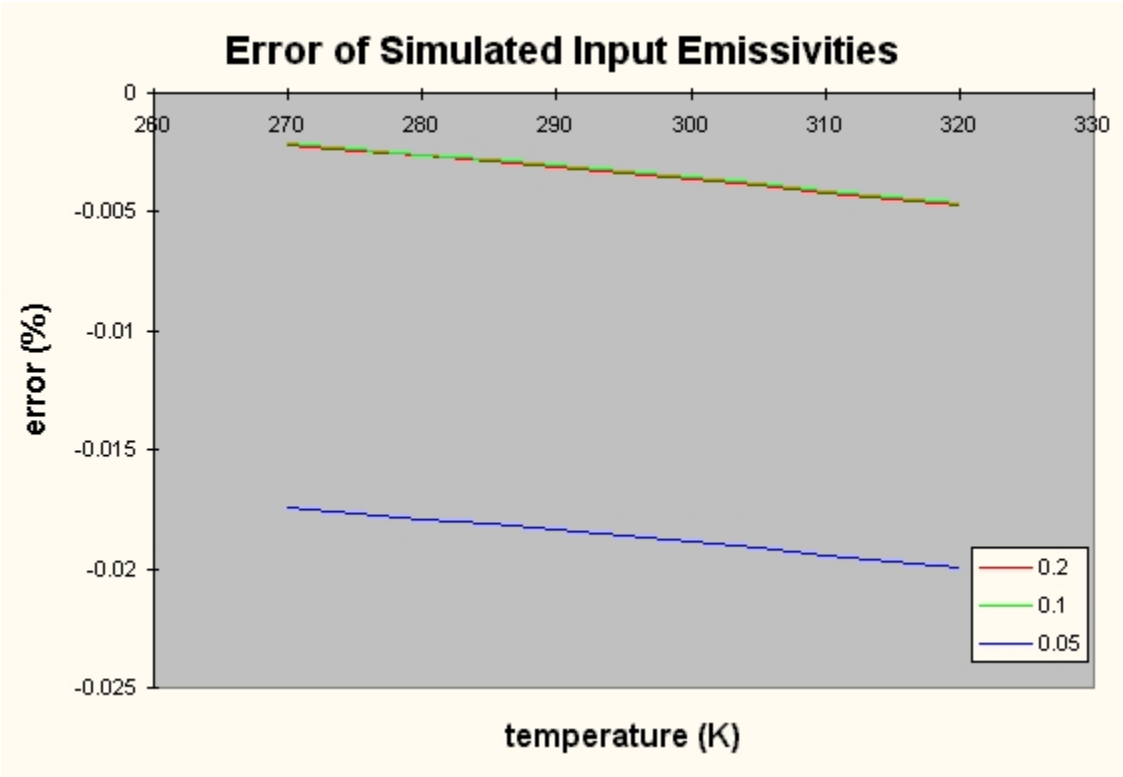

Figure 2: *Error of emissivity spectra with varying frequencies*

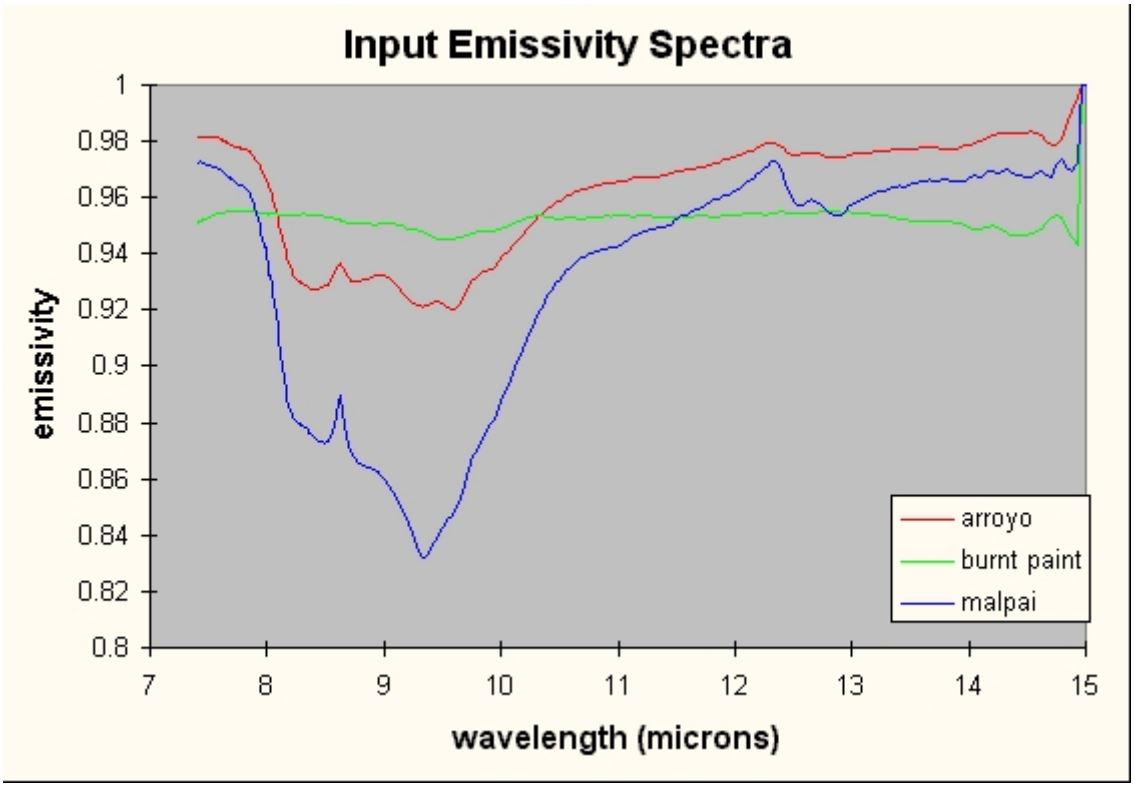

Figure 3: *Real input emissivity spectra*

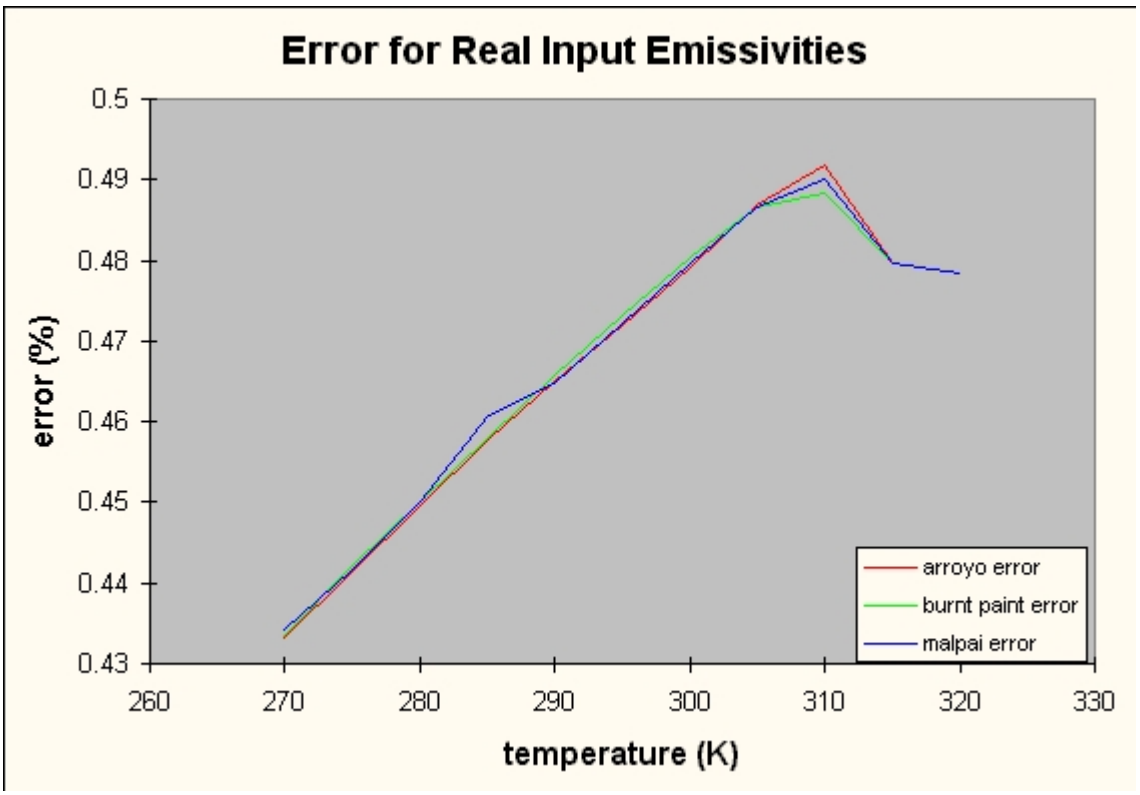

Figure 4: *Error as a function of temperature for real emissivity spectra.*

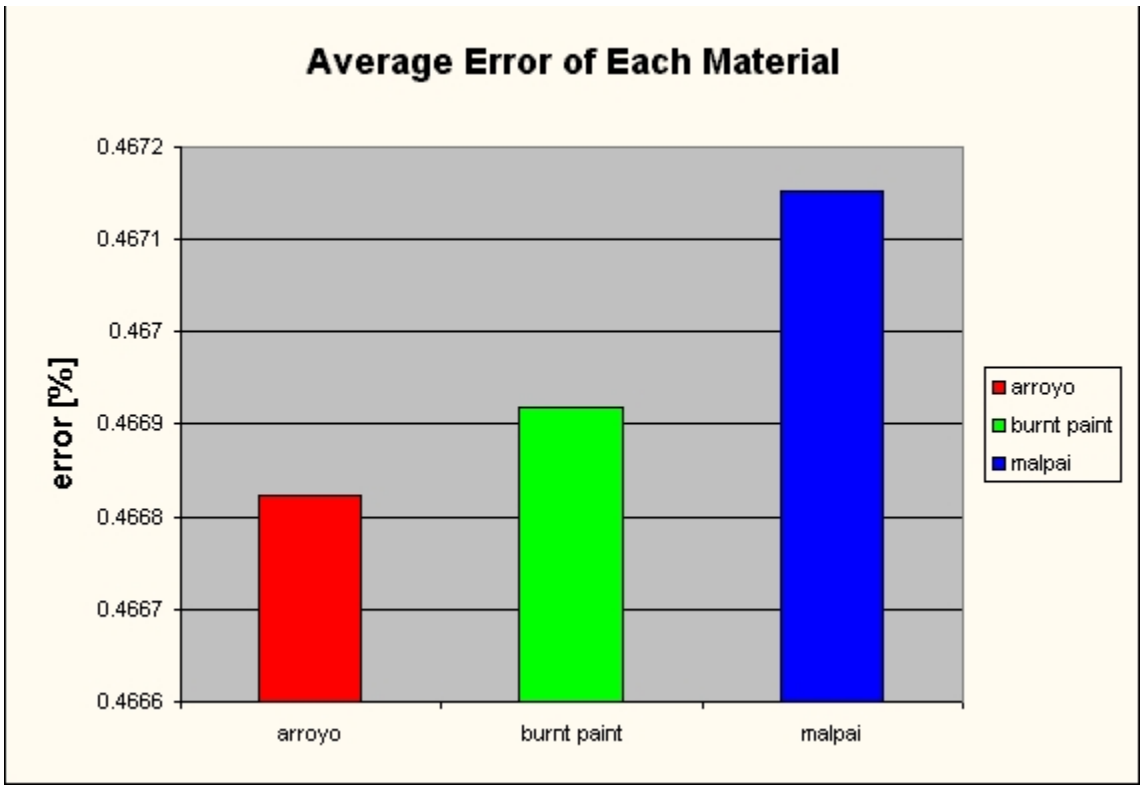

Figure 5: *Error of each material averaged across all temperatures (total error).*

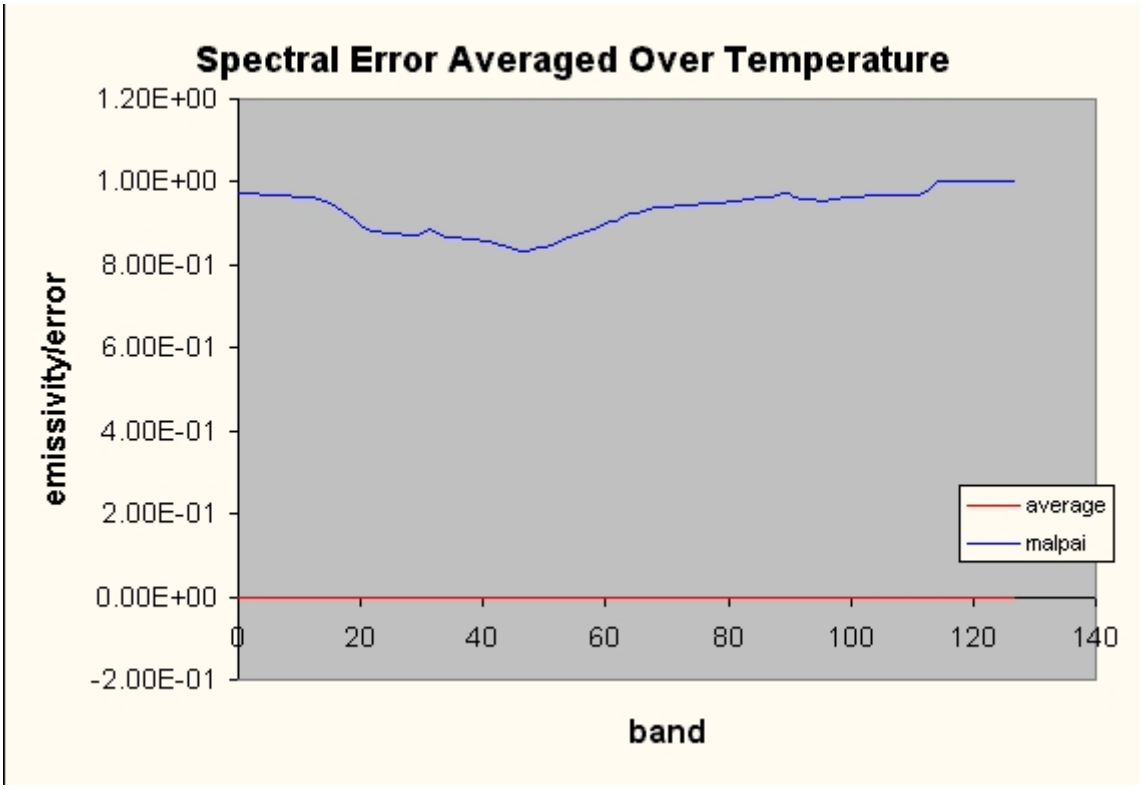

Figure 6: *Malpai spectrum compared to its average spectral error.*

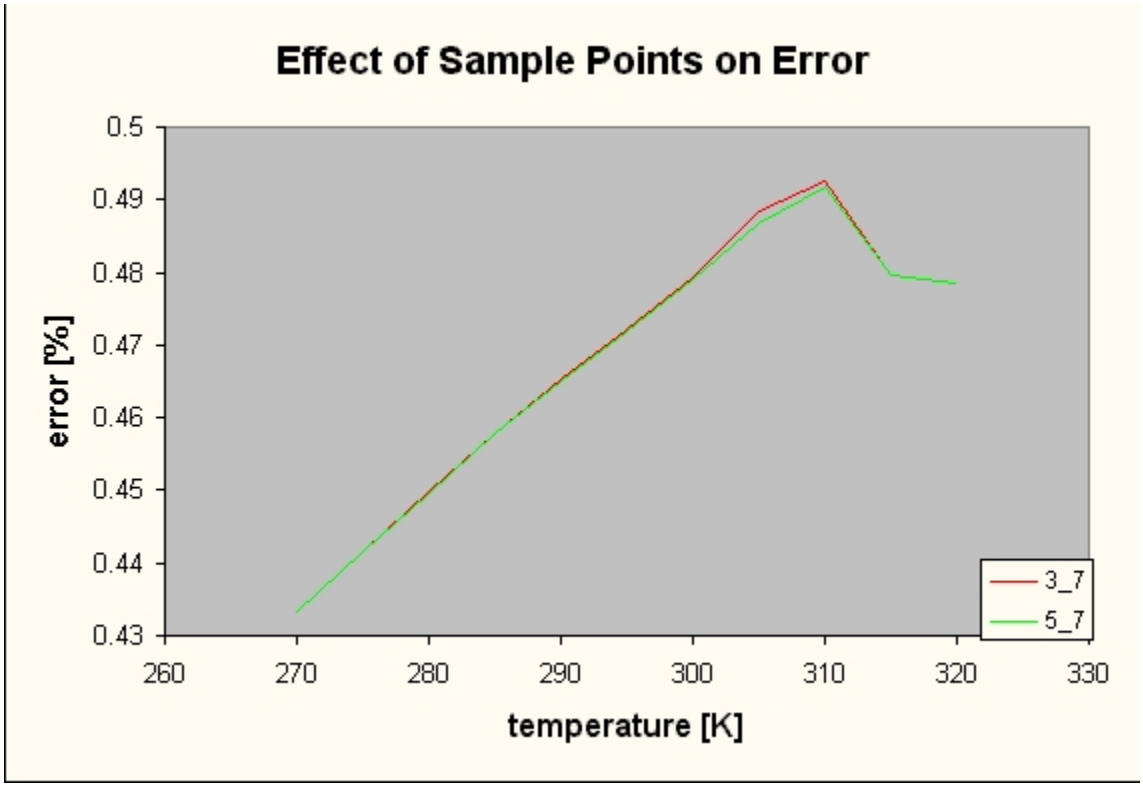

Figure 7: *Effect on error of changing sample points per channel with same response width.*

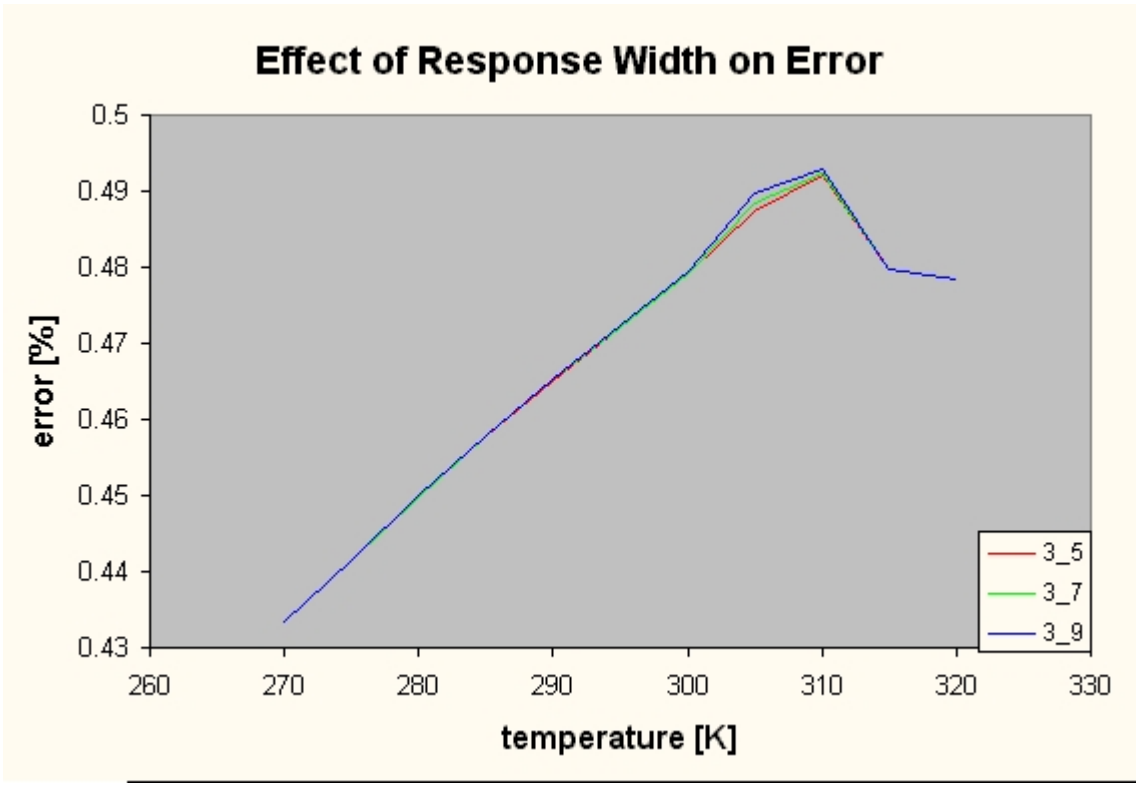

Figure 8: *Effect on error of varying response width with constant sample points.*

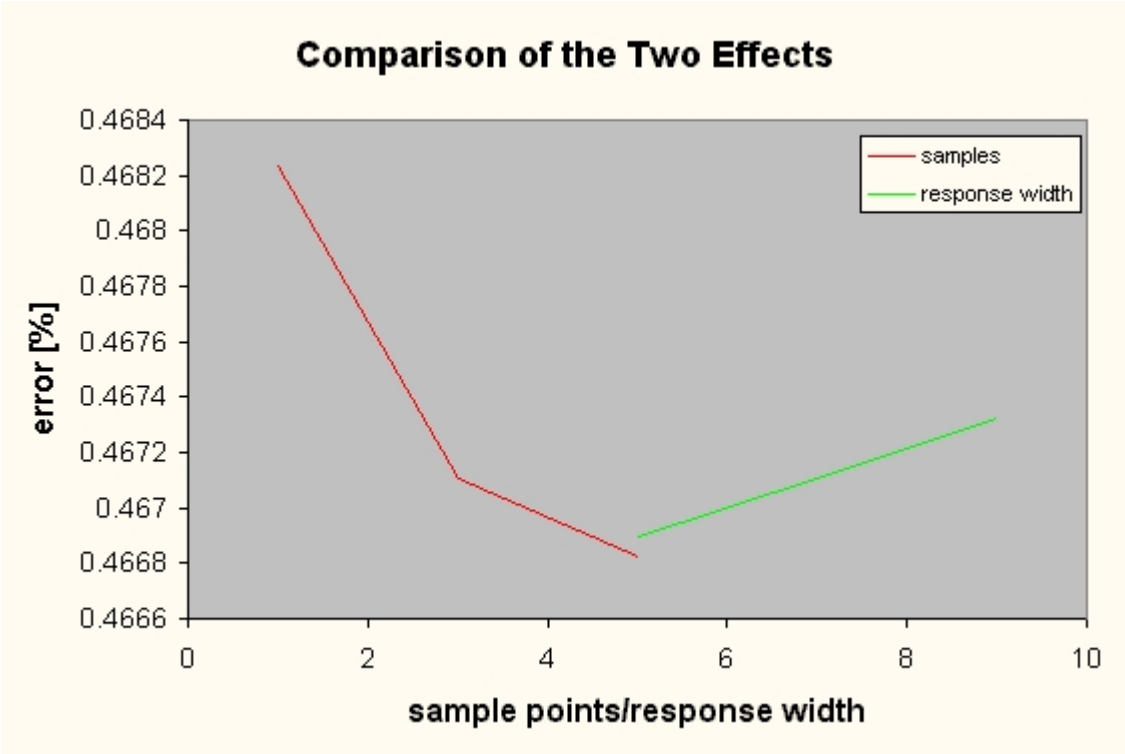

Figure 9: *Comparison of the effect of sampling and response width on error.*

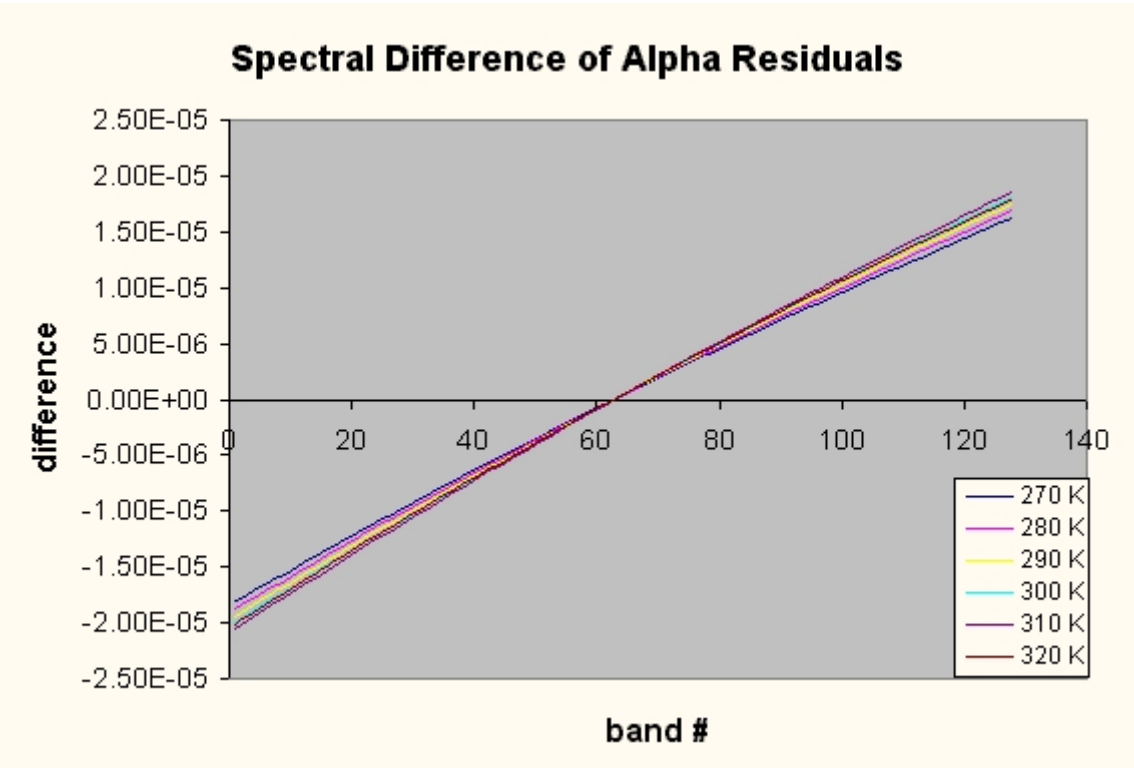

Figure 10: *Spectral difference of input and library alpha residual spectra at varying temperatures.*

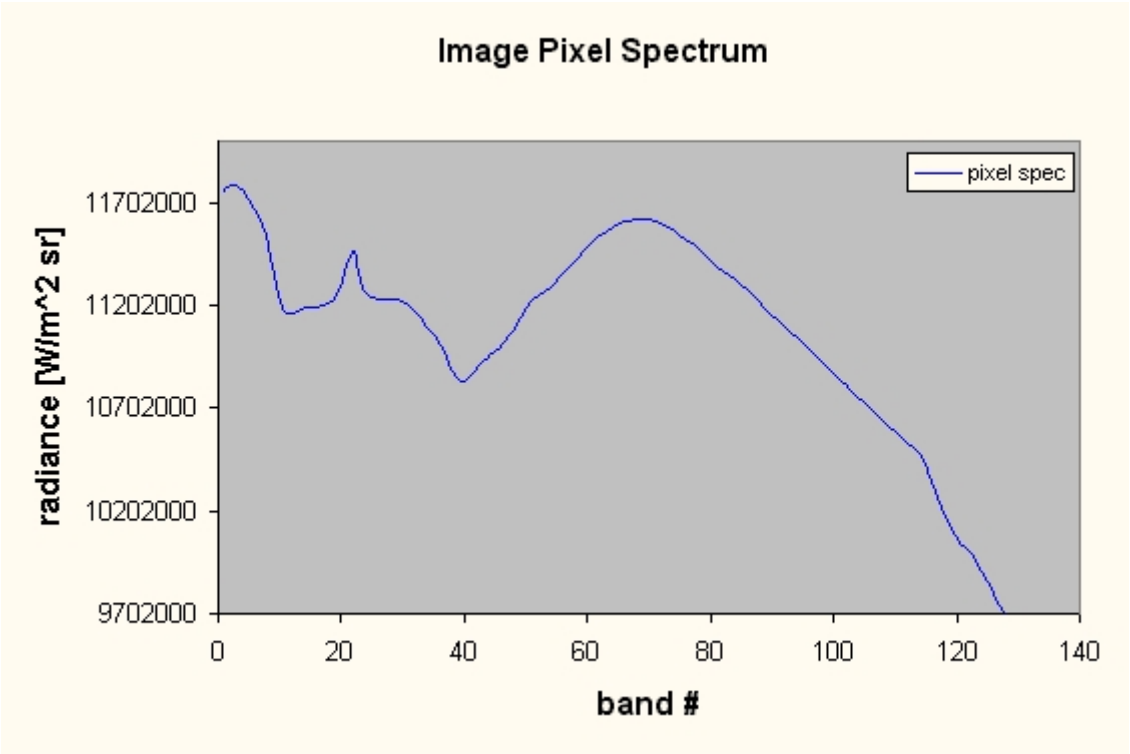

Figure 11: *Input spectrum of actual image pixel. The material is malpai.*

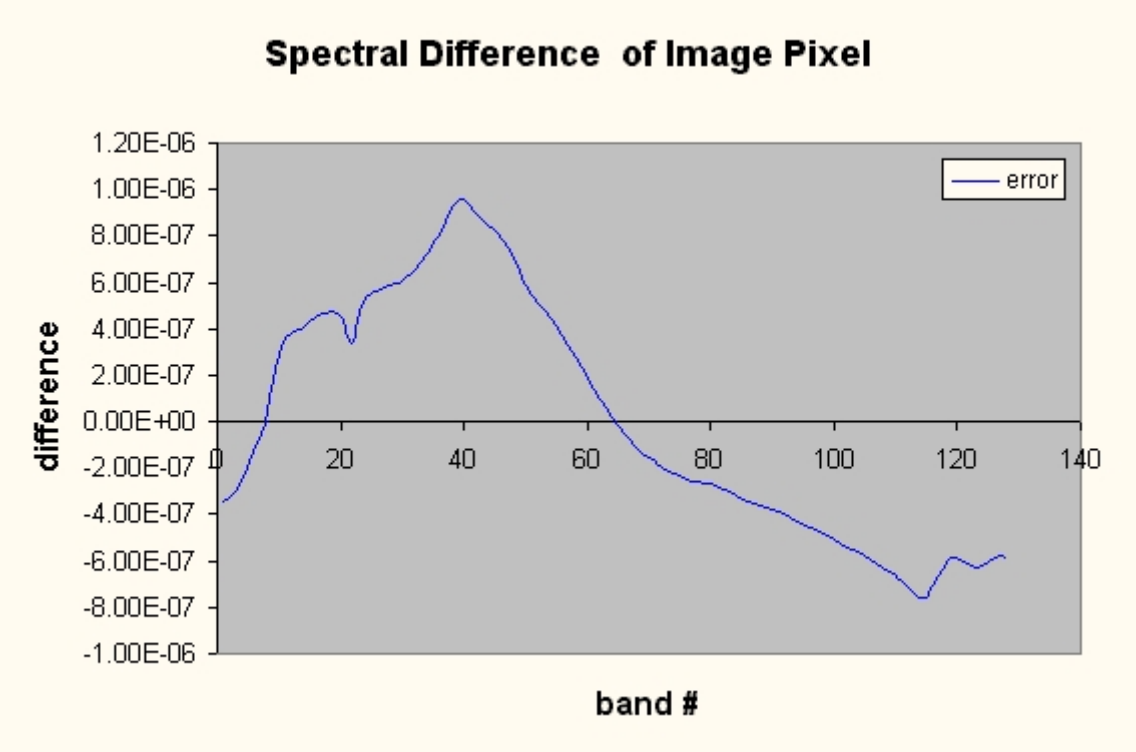

Figure 12: *Error spectrum of image and library alpha residuals. Notice the spectral structure.*

Discussion

The previous sections summarized the findings of this study. The first plot, Figure 1, is a representation of the three pseudo-emissivity curves used to simulate input data for the frequency study. Frequency of the curve is represented in the numbers in the legend.

Figure 2 show the error effects due to frequency. As you can see, 0.2 and 0.1 frequency spectra yield an error that is almost identical. The 0.05 frequency spectrum, however, yields a somewhat significant difference in error relative to the 0.2 and 0.1 curve. However, since the change is over such a small range, frequency effects can be viewed as negligible.

Real input emissivity spectra are shown in Figure 3. The three materials are arroyo, malpai, and burnt paint. Arroyo and malpai are desert soils. These are assumed to be perfectly corrected for atmospheric effects. Resolution of these files affected the error output. When they were obtained, these files had no where near the spectral resolution necessary to carry out the desired tests. To remedy that, an interpolator program was written to compute values between two points.

Error of actual input emissivities is shown in Figure 4. Each material has a unique error spectrum, but as you can see, they are still very similar. All the error points at each temperature are at about 0.45%, which is a significant improvement from the 1% error this algorithm demonstrated with TIMS data.

Figure 5 shows the total error of each material. This was computed by averaging the error at each temperature. Once again, on the graph, it looks like there are significant differences in the error for each material, but upon further inspection, you will notice that the range over which these changes occur is extremely small. Thus, it can be concluded that regardless of what material you're looking at, this algorithm will yield comparable results. No modifications need to be made as you look at different materials. It should be noted that in all the tests, each material exhibited the same trends. Output spectra were nearly identical with differences occurring at the fourth or fifth decimal place.

The next plot compares input and output. Figure 6 plots the malpai emissivity spectrum against the average of the alpha residual spectrum difference at each temperature. Due to how it is scaled, the real shape of the error cannot really be seen. It is a line of positive slope, but doesn't ever get to far away from the x axis. This plot shows us that in our simulations, there is no spectral structure in the error whatsoever.

Figure 7 represents the effect of sample points on error. The two lines plotted are the error of a 3 point sampling with a spectral response width of 7 and a 5 point sampling with a spectral response width of 7. Spectral response width was kept constant because only sample point effects were desired. It shows us that error increases as sample points decrease especially over the 300 -310 K range.

Response width was varied from plot to plot in Figure 8. Sample points were kept constant and response width was varied to 5, 7, and 9. The largest difference was seen over the same temperature range as the previous graph. Error increased with spectral response width. This is due to the fact that by increasing your spectral response width, you are effectively averaging photons into your data that come from adjacent spectral channels.

A comparison of sample points per channel and spectral response width effects are seen on Figure 9. At sample point values greater than 1, the error yielded quickly decreases due to the averaging that occurs across the channel. This provided a more accurate effective emissivity value for that channel, hence the decreased error. Error due to spectral response width increased linearly with width.

Figure 10 shows the spectral difference between the alpha residuals from the input emissivity spectra and the library alpha residual spectra. These differences are taken at temperatures ranging from 270K to 320K. Again, notice that there is no spectral structure in the error and that this behavior is exhibited from material to material. By averaging all these plots, a general correction can be obtained over all temperatures. If the image alpha residuals were adjusted by the inverse of the average error spectrum, i.e. if band 1 had an alpha residual difference of -1.5e-5, then that amount should be negated and added to band ones alpha residual. Upon this correction, the resulting error would be reduced to the width of the line. This hasn't been proven in this study, but data suggests that it is a feasible solution.

The final result obtained is from actual image data. Actual image data introduces noise and atmosphere into your input, so the error may be effected. Figure 11 represents the spectrum of the input pixel. The value being read in is actually the integrated radiance being computed in the simulations. Malpai is the material represented.

Figure 12 represents the spectral difference in the alpha residuals of the image and the library spectrum. Contradictory to our simulation results, it shows some spectral content over the first half of the spectrum. The spectral features of the error are inverted compared to the input. Error is on the order of e-7, so the results are promising.

Experimental error could have been introduced into this experiment in a variety of fasions. The

cause first and foremost in my mind is resolution of data files. Sample points at different wavelengths in the data files didn't match up with the ideal spatial sampling in the code. For this reason, the program computed the ideal wavelength to take data at and then proceeded to pick the nearest value in the file to which it corresponds. This may have thrown our results off because as wavelength changes, so do corresponding radiance and emissivity values. Perhaps this was the cause of the lack of spectral structure in the simulated error. Another cause of error is the modeling of the spectral response curves. Spectral responsivity was modeled to be approximately gaussian over the channel with some degree of overlap onto the adjacent channels. It is in the approximation of the width and point at which they overlap where error may have been introduced.

Conclusions

Based on the results obtained, I believe the original stated hypothesis is supported. While simulations showed no spectral structure in the error, they showed basic trends regarding the shape and magnitude of error spectra that lead to the belief that indeed a general error correction can be applied. With real image data providing output error somewhat related to input spectrum magnitude, it contradicted the findings of the simulations. However, the results from the real image data have not yet been validated and it is suggested that future work vigorously pursue this. Unfortunately, I was only able to analyze one pixel from one image. Although the validity of a general correction application may not be concrete, data strongly suggests its implementation. With continued research in the area, tests can verify its likelihood to be functional in real applications.

In addition to findings about the error correction possibilities, there are other things that have been learned from this research. First that the increased spectral resolution of the SEBASS sensor does in fact cut the error in half from TIMS data, with TIMS error being at about 1% and SEBASS at about 0.45%. Also, sampling and response width contribute to error. As spectral response width increases, so does error, and as sampling increases, error decreases.

Table of Contents

Error Characterization of the Alpha Residuals Emi ssivity Extraction Technique

Michael C. Baglivio

References

---

1. 1) Gillespie, A.R., Rokugawa, S., Hook, S.J., Matsunaga, T., Kahle, A.B. Temperature/Emissivity Separation Algorithm Theoretical Basis Document, Version 2.3 *Prepared under NASA contract NAS5-31372*, August 1996

2. 2) Schott, John *Remote Sensing: The Image Chain Approach*, Oxford University Press, New York, NY 1997

3. 3) Hook, S.J., Gabell, A.R., Green, A.A., Kealy P.S. A Comparison of Techniques for Extracting Emissivity Informatin from Thermal infrared Data for Geologic Studies, *Remote Sensing of Environment*, Volume 42, pp. 123-135, 1992

Table of Contents | Title Page

Error Characterization of the Alpha Residuals Emi ssivity Extraction Technique

Michael C. Baglivio

```
/*************************************************************************


TITLE: alpha_resid.c

BY: Mike Baglivio

CLASS: Senior Research


PURPOSE: To characterize error associated with Weins Approximation

in the alpha residuals T/e separation technique.


*************************************************************************/

#include<iostream.h>

#include<fstream.h>

#include<stdlib.h>

#include<math.h>


#define Y_SIZE 5

#define X_SIZE 5

#define NUM_BANDS 128


const double Pi = 3.141592654;

const double h = 6.634E-34;

const double k = 1.38054E-23;

const double c = 3.0E+8;

const double con1 = 2*Pi*h*c*c;
```

```
const double con2 = c*h/k;

const int n = 128;

const long int input_data_points = 35350;


int main(int argc, char *argv[])

{


//PROMPTS USER FOR NECCESSARY INPUT


int sub_sample;

char outfile[20];

int width;

int temp = 300;

cout<<"Use ODD numbers for sample points and response width."<<endl;

cout<<"How many sample points per channel?> ";

cin>>sub_sample;

cout<<"How wide would you like the spectral response curves to be?> ";

cin>>width;

cout<<"Output file name> ";

cin>>outfile;


//DEFINES START WAVELENGTH OF SAMPLE_WAVE ARRAY


long int i;

int j;

int q=0;

double wave_incr = .04e-6;
```

```
double init_w_val = 7.80e-6;

double w_val = 7.80e-6;



//DEFINES SUBSAMPLING AND INTERVAL FOR SAMPLE POINTS IN EACH CHANNEL


int sample_points = sub_sample*n + (width-sub_sample);

double sub_sample_incr = wave_incr/sub_sample;

double *sample_wave = NULL;

sample_wave = new double[ sample_points ];



//CREATES OUTPUT FILE


ofstream fout(outfile);


//READS INPUT IMAGE FILE


int x, y;

static float spectrum[ NUM_BANDS ];


/* open the image file */

ifstream input_file( "test.img" );


if(!input_file){

cerr<<"Image file cannot be opened" <<endl;

exit(1);
```

```
}

for( y = 0; y <1/*Y_SIZE*/; y++ ) {

for( x = 0; x <1 /*X_SIZE*/; x++ ) {

input_file.read( spectrum, sizeof( float ) * NUM_BANDS );

//input_file.close();



//LOOP FOR LIBRARY CALCULATION

int file=0;

for(file=1; file<argc; file++){

//fout<<argv[file]<<endl;

q=0;

double wave_incr = .04e-6;

double init_w_val = 7.80e-6;

double w_val = 7.80e-6;



//PRODUCES GAUSSIAN CURVE TO MODEL RESPONSIVITY

double *gauss = NULL;

gauss = new double[ width ];

double g=0;
```

```
for(i=0; i<width; i++){
g=pow(Pi*(i-(width-1)/2),2);
gauss[i]=exp(-g/100);
}

//CALCULATION LOOP
int *center = NULL;
center = new int[ n ];
int a;

for(i=0; i<n; i++){
center[i]=(i*sub_sample)+(sub_sample-1)/2; //center of band
for(j=0; j<width; j++){
a=center[i]-(width-1)/2+j;
if(a<0)
a=0;
if(a>sample_points)
a=sample_points;
}
}

//MAKES CALCULATIONS TO COMPUTE ALPHA RESIDUALS OF INPUT DATA

double *X_one = NULL;
X_one = new double[ n ];
double bandwidth[n]; //wave[n] is the bandwidth array
init_w_val=7.80e-6;
```

```
double sum_X_one=0.0;


for(i=0; i<n; i++){
bandwidth[i]=init_w_val;
init_w_val = init_w_val + wave_incr;
X_one[i]=bandwidth[i]*log(spectrum[i]);
sum_X_one+=X_one[i];
}
double X_one_bar=sum_X_one/n;
double *alpha_one = NULL;
alpha_one = new double[ n ];


for(i=0; i<n; i++){
alpha_one[i]=X_one[i]-X_one_bar;
}


//THIS SECTION COMPUTES ALPHA RESIDUALS OF THE LIBRARY SPECTRA


//READS IN LIBRARY EMISSIVITY FILE


double *library = NULL;
library = new double[ input_data_points ];
double *lib_wave = NULL;
lib_wave = new double[ input_data_points ];
double *actual_library = NULL;
actual_library = new double[sample_points];
double *actual_lib_wave = NULL;
```

```
actual_lib_wave = new double[sample_points];


ifstream fin(argv[file]);
if(!fin){
cerr<<"File cannot be opened" <<endl;
exit(1);
}


i=0;
while(fin >>lib_wave[i]>>library[i]){
i++;
}
fin.close();


//CONVERTS LIB_WAVE[I] INTO MICRONS


for(i=0; i<input_data_points; i++){
lib_wave[i] = lib_wave[i]*10e-6;
}


//EXTRACTS OUT NECESSARY WAVELENGTH AND EMISSIVITY VALUES FROM INPUT DATA


for(i=0; i<sample_points; i++){
sample_wave[i]=w_val;
w_val = w_val + sub_sample_incr;
for(j=0; j<input_data_points; j++){
if(lib_wave[j]>=sample_wave[i] && lib_wave[j]<sample_wave[i]+0.0001){
```

```
actual_lib_wave[i] = lib_wave[j];
actual_library[i] = library[j];
}
}
}
//COMPUTES EFFECTIVE EMISSIVITY

double e_num;
double e_denom;
double *eff_emmiss = NULL;
eff_emmiss = new double[ n ];
double *X_two = NULL;
X_two = new double[ n ];
double sum_X_two=0.0;
int z=0;

for(i=0; i<n; i++){
e_num=e_denom=0.0;
for(j=0; j<width; j++){
z=center[i]-(width-1)/2+j;
if(z<0)
z=0;
if(z>sample_points)
z=sample_points;
e_num+=actual_library[z]*gauss[j]*wave_incr;
e_denom+=gauss[j]*wave_incr;
}
```

```
eff_emmiss[i]=e_num/e_denom;

X_two[i]=bandwidth[i]*log(eff_emmiss[i])+bandwidth[i]*log(con1)-5*bandwidth[i]*log
(bandwidth[i])-bandwidth[i]*log(Pi)-con2/temp;

sum_X_two+=X_two[i];

//cout<<eff_emmiss[i]<<endl;

}



double X_two_bar=sum_X_two/n;

double *alpha_two = NULL;

alpha_two = new double[ n ];



for(i=0; i<n; i++){

alpha_two[i]=X_two[i]-X_two_bar;

//cout<<alpha_two[i]<<endl;

}



//COMPUTES DIFFERENCE OF INPUT AND LIBRARY SPECTRA



double difference;

double sum_diff=0.0;

double spec_diff=0.0;



for(i=0; i<n; i++){

sum_diff+=(alpha_two[i]-alpha_one[i])/alpha_two[i];

spec_diff=alpha_two[i]-alpha_one[i];

fout<<spec_diff<<endl;

}
```

```
difference=sum_diff/n;




} //END OF LIBRARY LOOP


//cout<<min<<endl;

}

}

return(0);

}
```